17
Random Lasing in Solid State Materials

J. Fernández, R. Balda, S. García-Revilla, J. Azkargorta, and I. Iparraguirre

17.1 Introduction

In 1967, Letokhov theoretically predicted the possibility of generating laser-like emission starting from scattering particles with negative absorption, the so-called *random* or *powder laser*. Random lasers are the simplest sources of stimulated emission without cavity, with the feedback provided by disordered-induced light scattering due to spatial inhomogeneity of the medium [1]. The specific feedback mechanism and behaviour of a given system depends on its particular nature and morphology. A detailed discussion about the latest results and theories concerning the mechanisms responsible for random lasing and the precise nature of the random laser modes can be found in Refs. [2–6].

Since 1986 when Markushev et al. demonstrated laser-like behaviour in a powder of $Na_5La_{1-x}Nd_x(MoO_4)_4$ at liquid nitrogen temperature [7], similar random laser experiments have been conducted at room temperature in numerous Nd-doped pulverized materials and highly scattering Nd-doped ceramics. The history and the state of the art of these neodymium-activated random lasers are reviewed by Noginov in Ref. [3]. Among these materials, the stoichiometric $NdAl_3(BO_3)_4$ powder was regarded as a promising room temperature solid-state random laser material [8] because it presents many desirable features, such as a low laser threshold, a high gain, high Nd^{3+} concentration, and excellent physical and chemical properties [9, 10].

J. Fernández (✉) • R. Balda • S. García-Revilla • J. Azkargorta • I. Iparraguirre
Dpto. Física Aplicada I, Escuela Superior de Ingenieria, Universidad del País Vasco UPV/EHU, Alda. Urquijo s/n, Bilbao 48013, Spain

J. Fernández • R. Balda
Materials Physics Center CSIC-UPV/EHU and Donostia International Physics Center, San Sebastian 20080, Spain
e-mail: joaquin.fernandez@ehu.es

B. Di Bartolo et al. (eds.), *Nano-Optics for Enhancing Light-Matter Interactions on a Molecular Scale*, NATO Science for Peace and Security Series B: Physics and Biophysics, DOI 10.1007/978-94-007-5313-6_17,

We present here the random laser performance of ground powders of the yttrium borate family, $Nd_xY_{1-x}Al_3(BO_3)_4$ ($x = 0.5–1$). In particular, the dependence of their random laser threshold, slope efficiency, and emission kinetics on the Nd^{3+} concentration. Although the obtained results are qualitatively similar in all the explored powders, our findings show a reduction of the onset of laser-like emission and an increase of the slope efficiency when increasing the Nd^{3+} content [11]. At a first glance this behaviour seems to be unexpected due to the luminescence quenching at high concentrations; however, account taken of the short build up time of the random laser pulses, the lifetime shortening of the excited state, as concentration increases, does not affect the random laser process. It is therefore clear that for a random laser material high effective gain within the build up time scale of the pulse construction is the important issue. Following these results, we have looked for alternative crystal laser materials having higher stimulated emission cross-sections than borates and which could allow using low rare-earth concentration doping but keeping the effective gain still optimal for random laser operation. Among those possible candidates Nd-doped orthovanadate crystals have been proved to be efficient laser materials for diode-pumped solid state lasers due to their large absorption and emission cross sections, high chemical stability, and high damage threshold. Among vanadates Nd^{3+}:$LuVO_4$ has attracted much attention since it has the highest absorption and emission cross-sections, 6.9×10^{-19} cm^2 at 808 nm and 14.6×10^{-19} cm^2 at 1.06 μm respectively. Moreover, the relevance of Nd^{3+}:$LuVO_4$ crystal has been recently confirmed by the demonstration of passively Q-switched laser-diode pumped nanosecond self-Raman laser operating at cascade downconverted frequency [12].

Here we show the most relevant features of the random lasing action both in the spectral and temporal domains of a low concentrated Nd^{3+}-doped lutetium vanadate powder [13]. Laser threshold and emission efficiency were comparable to those obtained in stoichiometric borate crystal powders obtained under the same focusing and measuring conditions.

17.2 Experimental

17.2.1 Synthesis and Characterization of the Powder Laser Samples

Polycrystalline powders of $Nd_xY_{1-x}Al_3(BO_3)_4$ ($x = 0.5$, 0.6, 0.7, 0.8, 0.9, and 1) have been prepared at the Materials Science Institute of Madrid by Prof. Cascales group. The laser materials were ground afterwards by using a mixer mill. The polydispersity of the resulting powder was evaluated from scanning electron microscope photographs. The average particle size was 4 ± 2 μm, similar for all samples. All the ground powder samples were compacted in quartz cells without

a front window for handling ease and optical characterization. The volume filling factor of the powder materials ($f = 0.39$) was calculated by measuring sample volume and weight.

The Nd^{3+}-doped lutetium vanadate single crystals utilized in the random laser experiments presented in this work were grown at the University of Verona by Prof. M. Bettinelli group by using spontaneous nucleation in a $Pb_2V_2O_7$ flux [14]. The Nd^{3+} concentration in the sample used for random laser experiments was 3 mol%. The polydispersity of the measured powders was also evaluated from SEM photographs. The average particle size was 3 ± 2 μm.

17.2.2 Experimental Techniques

The random laser experiments were performed at room temperature in a backscattering arrangement by using a Ti-sapphire laser pumped by a pulsed frequency doubled Nd: YAG laser (9 ns pulse width) as the excitation source. The pump beam diameter on the sample surface was varied from 0.3 to 4 mm. The emission from the front face of the samples was collected with an optical fiber by use of two lenses. A long-pass filter was used to remove light at the pump wavelength. In the spectral measurements, the emitted light was dispersed by a 0.25 m monochromator and detected with a photomultiplier coupled to a boxcar integrator. The emission kinetics traces were recorded by using a fast photodiode connected to a digital oscilloscope (temporal resolution of 400 ps).

17.3 Random Laser Performance of $Nd_xY_{1-x}Al_3(BO_3)_4$ Laser Crystal Powders

In this section, the optimum neodymium concentration and focusing conditions in order to reduce the random lasing threshold pumping density in yttrium borate compounds are presented. Moreover, the dependence of the output slope efficiency on the Nd^{3+} concentration is investigated.

We experimentally analyzed the spectra and emission dynamics of $Nd_xY_{1-x}Al_3(BO_3)_4$ ground powders when increasing the excitation energy. At low pumping energies, these laser crystal powders show only regular spontaneous emission with a single exponential emission kinetics. Figure 17.1 shows the normalized spontaneous emission spectrum (dashed line) of the $NdAl_3(BO_3)_4$ powder at the $^4F_{3/2} \rightarrow {}^4I_{11/2}$ transition. This spectrum was measured at 4 mJ/pulse, with a pump beam diameter on the sample of 1.87 mm. The lifetime of the Nd^{3+} upper laser level $^4F_{3/2}$ (determined by its spontaneous emission decay) is reduced from 15.6 μs in the less concentrated sample ($x = 0.5$) to 12.7 μs for the stoichiometric sample. Similar concentration quenching of the Nd^{3+} lifetime is observed in other

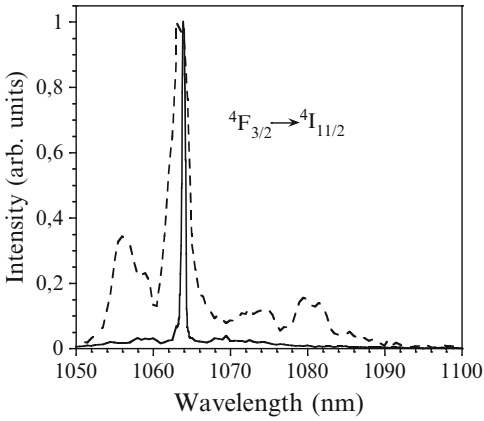

Fig. 17.1 Normalized emission spectra of the $NdAl_3(BO_3)_4$ powder obtained pumping at 802 nm with a pump spot size of 1.87 mm. The *dashed* and *solid lines* correspond to the fluorescence and laser-like emission spectra measured below and above the threshold at 4 mJ/pulse and 20 mJ/pulse, respectively

neodymium-doped laser materials. On the other hand, with the increase of the pumping energy, the amplified spontaneous emission of the laser crystal powders increases causing an enhancement of the emission intensity and a non exponential nature of the emission dynamics. In particular, above a certain critical threshold value both the spectra and the kinetics of Nd^{3+} luminescence change dramatically. The intensity of the strongest line in the spontaneous emission spectrum increases several orders of magnitude and its width becomes smaller. As evidenced in Fig. 17.1, the spectrum obtained at 20 mJ/pulse collapses to a narrow single line with a linewidth of 0.4 nm. It is worthy to remark that no spikes were observed in the laser-like emission spectra of our powder samples which suggests a nonresonant feedback mechanism of the explored random laser effect.

As mentioned before, just above the threshold energy the emission kinetics changes to a very short and intense emission pulse with a duration in the nanosecond time-scale (∼1 ns). At stronger pumping, a second emission pulse emerges in the kinetics, and as the pumping energy is increased, the number of stimulated emission pulses increases manifesting the typical laser relaxation behaviour. Notice that relaxation oscillations in random lasers have been theoretically predicted by Letokhov in 1968 [1] and studied more recently in detail [15 and references therein]. In neodymium random lasers, they occur in a highly nonlinear regime showing narrow stimulated emission pulses (∼1 ns) occurring during a much longer pumping pulse (∼10 ns) [10]. These oscillations are strong in the beginning of the lasing process and are damped at longer times. Moreover, the study of the kinetics of relaxation oscillations in random lasers reveals information about the photon residence time in the scattering medium [16]. Figure 17.2 shows the temporal evolution of the $NdAl_3(BO_3)_4$ powder emission recorded below the lasing threshold (2 mJ/pulse solid line), just above the lasing threshold (5 mJ/pulse dashed-dotted line), and well above the lasing threshold (15 mJ/pulse dashed line) with the same pump spot size used to measure the emission spectra. As can be observed, the delay time between the first emission pulse and the onset of the fluorescence becomes shorter as the excitation energy increases. The other laser crystal powders exhibited a qualitative similar behaviour.

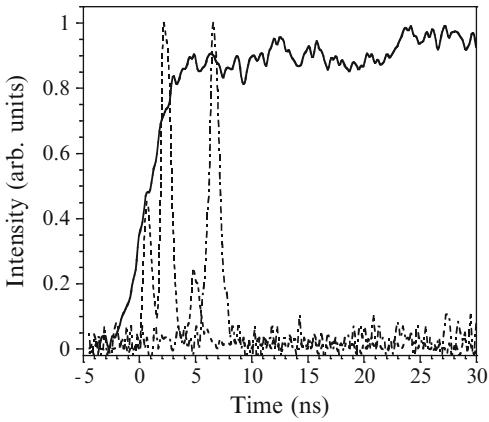

Fig. 17.2 Temporal evolution of the emission intensity of the $NdAl_3(BO_3)_4$ powder obtained at 2 mJ/pulse (*solid line*), 5 mJ/pulse (*dashed-dotted line*) and 15 mJ/pulse (*dashed line*) with a pump spot size of 1.87 mm ($\lambda_{exc} = 802$ nm)

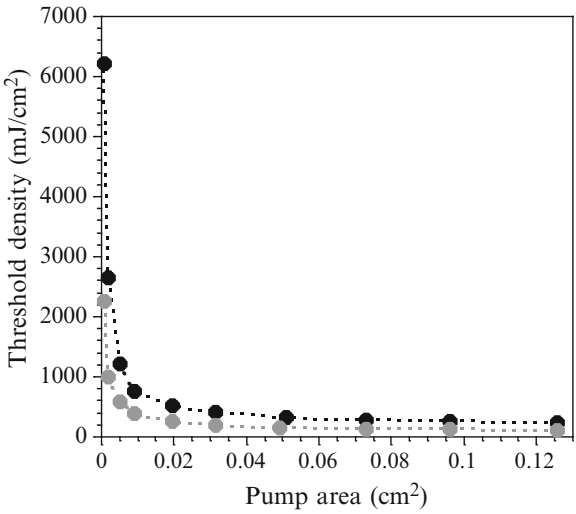

Fig. 17.3 Threshold pumping density of the $NdAl_3(BO_3)_4$ (*grey dots*) and $Nd_{0.5}Y_{0.5}Al_3(BO_3)_4$ (*black dots*) powder as a function of the pumped spot area ($\lambda_{exc} = 802$ nm)

We also explored the dependence of the random laser threshold energy of the $NdAl_3(BO_3)_4$ and $Nd_{0.5}Y_{0.5}Al_3(BO_3)_4$ laser crystal powders on the size of the pumped spot. Figure 17.3 depicts the threshold pumping density of both samples as a function of the pumped area. Both curves show the same behaviour but larger threshold values are found in the non-stoichiometric borate powder. As can be observed, the threshold pumping density sharply increases at rather small areas of the pumped spot (where damage of the powder laser material can also occur at high pumping energies). In order to explain this result, one should take into account that (1) gain spatial distribution is governed by the spreading of pump light in the powder, and (2) light is emitted in the pumped region of the powder from where it starts to diffuse. For small excitation beam sizes, the light paths will very probably leave the amplifying or pumped volume after a short time, with a small chance to return. This implies that the threshold pumping density should be high

as a large gain is needed to compensate losses. With the increase of the size of the pumped spot, the amplifying volume increases. Therefore, photon walk paths elongate as light can travel longer inside the gain volume and can be more strongly amplified. Furthermore, if the photon leaves the gain volume and reaches the passive (unexcited) part of the powder, it could have a higher chance to return back to the amplifying region because of the larger excited volume. Consequently, a reduction of the random laser threshold density is expected in such a case. Nevertheless, as evidenced from Fig. 17.3, the threshold pumping density is almost independent of the pump spot area at large diameters. This behaviour can be explained regarding the flat-disk geometry of our pumping (the pump beam diameter, d, is larger than the penetration depth, which is typically less than 60 μm in neodymium random lasers at 532 nm [16]). Note that as $d \to \infty$ the number of paths per unit area of the pumped spot with a greater enough length to produce laser-like emission does not increase infinitely, but rather it will saturate at some constant value accounting for the saturation behaviour presented in Fig. 17.3 [17]. The same threshold trend with the pump beam size was experimentally observed in other neodymium doped materials [17]. It is worthy mentioning that the condition for the diffusion approximation ($\lambda << l_t << L$, where λ is the pump wavelength and L is the scattering sample thickness) is satisfied in the explored powder samples as l_t was estimated to be around 9.3 μm in the $NdAl_3(BO_3)_4$ and nonstoichiometric powders at the excitation wavelength ($\lambda = 802$ nm).

It is also clear from Fig. 17.3 that the Nd^{3+} concentration strongly influences the onset of laser-like emission. By measuring the input-output curves of the $Nd_xY_{1-x}Al_3(BO_3)_4$ laser crystal powders, we studied the Nd^{3+} concentration effect on the random laser performance of this yttrium borate family. Figure 17.4 shows the time integrated output intensity of the random laser pulses versus pump pulse energy for Nd^{3+} concentrations between $x = 0.5$ and 1. A pump spot size of 2 mm was employed. As already mentioned, just above the threshold the emission intensity undergoes a dramatic increase which is linear with pump fluence making the threshold sharp and well defined. As in regular lasers, the linear fit of these curves provides not only the threshold value but also the slope efficiency of stimulated emission. The fits corresponding to each powder sample are also displayed in Fig. 17.4. Figure 17.5 shows the random laser threshold energies (black squares) and slopes (black diamonds) inferred from the linear fits of the experimental data depicted in Fig. 17.4. The grey points of Fig. 17.5 represent the critical energy value at which the emission kinetics of the different powder samples is shortened to one short pulse. The error bars of these data are due to the energy fluctuations of the Ti-sapphire pump laser. As expected, there is a good agreement between these energies and the threshold values obtained from the linear fit of the input-output curves (black squares). It is clear from Fig. 17.5 that despite the existence of some lifetime concentration quenching, the increase of the Nd^{3+} content in the yttrium borate family leads to a reduction of the random laser threshold and to an enhancement of the relative slope of the random laser emission. Note that under the focusing conditions described above, the threshold energy of the $Nd_{0.5}Y_{0.5}Al_3(BO_3)_4$ powder

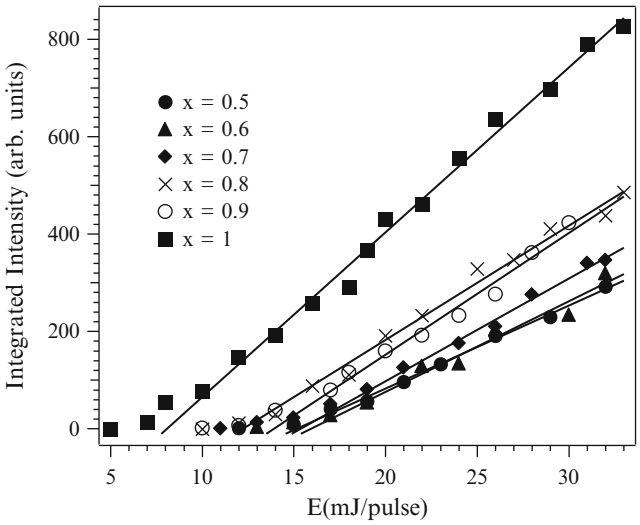

Fig. 17.4 Integrated area under the emission kinetics trace of the $Nd_xY_{1-x}Al_3(BO_3)_4$ ($x = 0.5$–1) powder as a function of the pump energy. *Dots, triangles, diamonds, crosses, circles*, and *squares* correspond to powder compositions with $x = 0.5$, 0.6, 0.7, 0.8, 0.9, and 1, respectively. *Solid lines* represent the linear fits of the experimental data. The diameter of the pump spot is 2 mm ($\lambda_{exc} = 802$ nm)

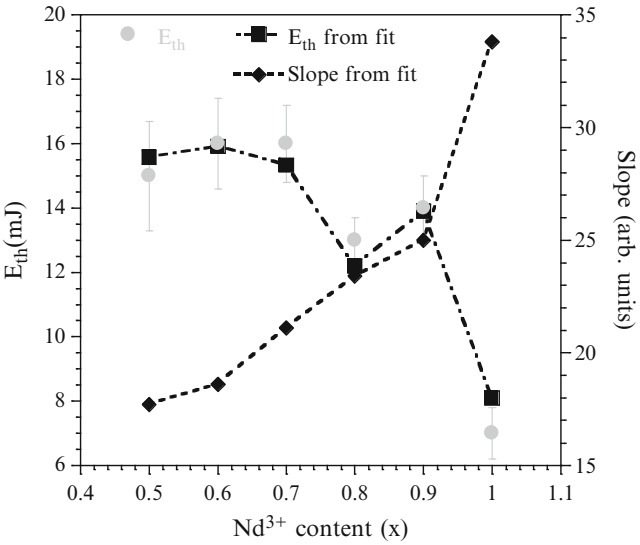

Fig. 17.5 Random laser threshold energy (*black squares*) and slope (*black diamonds*) values obtained from the linear fits of the input-output curves of the $Nd_xY_{1-x}Al_3(BO_3)_4$ powders as a function of the Nd^{3+} content. *Grey dots* correspond to the energy values at which their emission dynamics is shortened to one short pulse. The error bars represent the energy fluctuations of the pump laser

is about 15 mJ/pulse whereas the onset of laser-like emission in the $NdAl_3(BO_3)_4$ powder is around 7 mJ/pulse. Moreover, the stoichiometric powder has twice a larger slope efficiency than the former one.

17.4 Random Laser Performance of Nd^{3+}:$LuVO_4$ Crystal Powders

Figure 17.6 shows the emission spectra of the $^4F_{3/2} \rightarrow {}^4I_{11/2}$ transition of Nd^{3+} in the Nd^{3+}:$LuVO_4$ powder sample obtained at low (5 mJ) and high (24 mJ) pumping energies. At low pump energy the spectrum presents the typical spontaneous emission features with a main peak around 1,065.6 nm and some additional structures spreading over 10 nm. When increasing the pump energy, there is a threshold value of 9 mJ above which the emission peak intensity suddenly increases whereas the emission spectrum collapses to a narrow single line at 1,065.6 nm and 0.3 nm HWHM, our spectral resolution limit.

The emission kinetics parallels the spectral behaviour; at low pumping energy the spontaneous emission is single exponential with a decay time of 60 μs whereas above threshold the time profile shortens up and gives a fast emission pulse with a duration of about 800 ps. As pumping increases well above the threshold energy, more pulses appear in the emission temporal profile showing the typical laser relaxation oscillation behaviour. As can be seen in Fig. 17.7, we recorded, at maximum pump energy, up to six oscillations. As is common in conventional solid state lasers, the build-up time (time delay between the output pulses and the pumping pulse) of the random laser pulse decreases gradually as pumping energy increases. As its duration is about 10 ns, this figure clearly shows that the relaxation oscillations remain until the pump pulse is over.

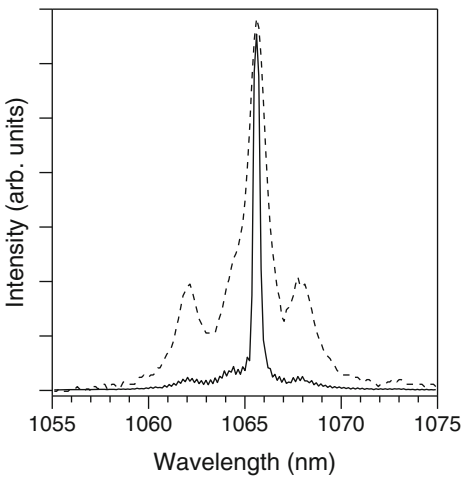

Fig. 17.6 Normalized emission spectra from Nd^{3+}(3%) $LuVO_4$ powder crystal obtained at pumping energies below (5 mJ *dashed line*) and above (24 mJ *solid line*) the laser threshold

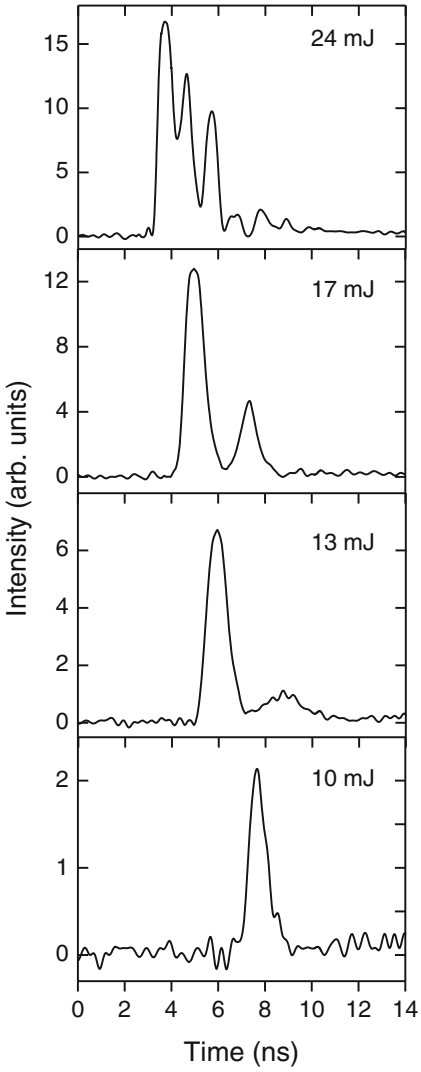

Fig. 17.7 Stimulated emission intensity pulses of Nd^{3+} (3%) :$LuVO_4$ powder crystal as function of time at some different pump energies. The zero time marks the start of the pump pulse

We have compared the random laser performance of this material with the one obtained in a ground laser powder of $NdAl_3(BO_3)_4$ under the same focusing and measuring conditions. To avoid damage in the vanadate sample surface the maximum pump energy used was 25 mJ (about 300 mJ/cm^2). The damage threshold in borate is at least one magnitude order higher.

Figure 17.8 shows the time integrated intensity of the output pulses from these powders as a function of the pumping energy. The laser threshold was obtained with pump pulses of about 9 mJ for both samples being the slope efficiencies similar but slightly higher for the vanadate sample. The origin of this similar random lasing behaviour relies on the different Nd^{3+} concentrations of both compounds.

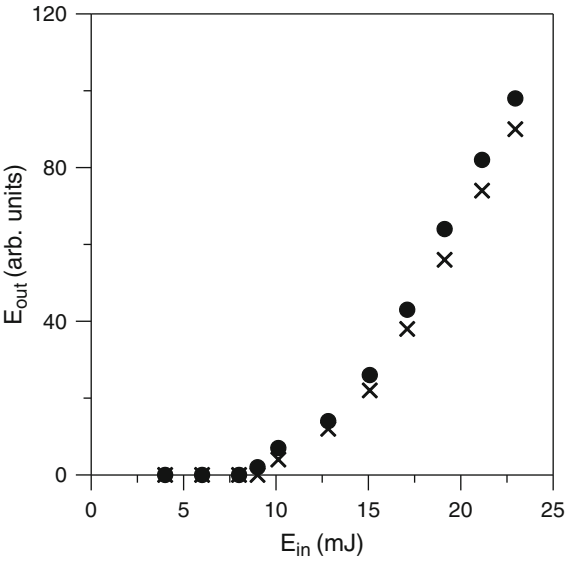

Fig. 17.8 Laser output energy as a function of the pumping energy for Nd^{3+}(3%):$LuVO_4$ (*dots*) and $NdAl_3(BO_3)_4$ (*crosses*) powders

Although the emission cross section in Nd-doped lutetium vanadate is higher than in the aluminium borate compound, $NdAl_3(BO_3)_4$ is a stoichiometric compound with higher Nd^{3+} concentration (around 20 times) than the 3% Nd^{3+}-doped $LuVO_4$ and therefore it is possible to obtain an "accidental" equalized gain for the random lasing emission. Moreover, although the focussing conditions were the same for both compounds, the pumped volume, and therefore gain, may be different due to the different neodymium concentrations and refractive indices of both compounds. These results therefore suggest that better random laser performances of the vanadate could be achieved with more concentrated powders as has already been demonstrated in Nd-doped borate crystal powders.

17.5 Conclusions

We have obtained random laser action in Nd^{3+}-doped yttrium borate and lutetium vanadate crystal powders. We have compared their random laser performances, under similar experimental conditions. Account taken of the similar performances obtained and the very different dopant concentration of both powders, the results open up the possibility of using these Nd-doped vanadates as efficient random laser sources.

Acknowledgements This work has been supported by the Spanish Government under Projects No. FIS2011-27968, MAT2009-14282-C02-02, Consolider SAUUL CSD2007-00013, and Basque Country Government (IT-331-07).

References

1. Letokhov VS (1967) Stimulated emission of an ensemble of scattering particles with negative absorption. JETP Lett 5:212–215
2. Wiersma DS (2008) The physics and applications of random lasers. Nat Phys 4:359–367
3. Noginov MA (2005) Solid-state random lasers. Springer, Berlin
4. Cao H (2003) Lasing in random media. Waves Random Media 13:R1–R39
5. Wiersma DS, Noginov MA (2010) Nano and random lasers. J Opt 12:020201
6. Andreasen J, Asatryan AA, Boten LC, Byrne MA, Cao H, Ge L, Labonté L, Sebbah P, Stone AD, Türeci HE, Vanneste C (2011) Modes of random lasers. Adv Opt Photon 3:88–127
7. Markushev VM, Zolin VF, Briskinia CM (1986) Luminescence and stimulated emission of neodymium in sodium lanthanum molybdate powders. Sov J Quantum Electron 16:281–283
8. Bahoura M, Noginov MA (2003) Determination of the transport mean free path in a solid-state random laser. J Opt Soc Am B 20:2389–2394
9. Xue D, Zhang S (1996) Calculation of the nonlinear optical coefficient of $NdAl_3(BO_3)_4$ crystal. J Phys Condens Matter 8:1949–1956
10. Noginov MA, Noginova NE, Caulfield HJ, Venkateswarlu P, Thompson T, Mahdi M, Ostroumov V (1996) Short-pulsed emission in the powders of $NdAl_3(BO_3)_4$, $NdSc_3(BO_3)_4$, and $Nd:Sr_5(PO_4)_3$ laser crystals. J Opt Soc Am B 13:2024–2033
11. García-Revilla S, Iparraguirre I, Cascales C, Azkargorta J, Balda R, Illarramendi MA, Al-Saleh M, Fernández J (2011) Random laser performance of $Nd_xY_{1-x}Al_3(BO_3)_4$ laser crystal powders. Opt Mater 34:461–464
12. Kaminskii AA, Bettinelli M, Dong J, Jaque D, Ueda K (2009) Nanosecond Nd^{3+}:$LuVO_4$ self-Raman laser. Laser Phys Lett 6:374–379
13. Azkargorta J, Bettinelli M, Iparraguirre I, Garcia-Revilla S, Balda R, Fernández J (2011) Random lasing in Nd:$LuVO_4$ crystal powder. Opt Express 19:19591–19599
14. Garton G, Smith SH, Wanklyn BM (1972) Crystal growth from the flux systems PbO–V_2O_5 and Bi_2O_3–V_2O_5. J Cryst Growth 13–14:588–592
15. Zhu G, Tumkur T, Noginov MA (2010) Anomalously delayed stimulated emission in random lasers. Phys Rev A 81:065801
16. Bahoura M, Morris KJ, Zhu G, Noginov MA (2005) Dependence of the neodymium random laser threshold on the diameter of the pumped spot. J Quantum Electron 41:677–685
17. Bahoura M, Morris KJ, Noginov MA (2002) Threshold and slope efficiency of $Nd_{0.5}La_{0.5}Al_3(BO_3)_4$ ceramic random laser: effect of the pumped spot size. Opt Commun 201:405–411